RSC Advances

This is an *Accepted Manuscript*, which has been through the Royal Society of Chemistry peer review process and has been accepted for publication.

Accepted Manuscripts are published online shortly after acceptance, before technical editing, formatting and proof reading. Using this free service, authors can make their results available to the community, in citable form, before we publish the edited article. This *Accepted Manuscript* will be replaced by the edited, formatted and paginated article as soon as this is available.

You can find more information about *Accepted Manuscripts* in the Information for Authors.

Please note that technical editing may introduce minor changes to the text and/or graphics, which may alter content. The journal's standard Terms & Conditions and the Ethical guidelines still apply. In no event shall the Royal Society of Chemistry be held responsible for any errors or omissions in this *Accepted Manuscript* or any consequences arising from the use of any information it contains.

ROYAL SOCIETY OF CHEMISTRY

www.rsc.org/advances

Cite this: DOI: 10.1039/c0xx00000x

www.rsc.org/xxxxxx

ARTICLE TYPE

Low-temperature solution growth of textured zinc oxide films for light trapping enhancement in thin film silicon solar cells

Chao-Ping Liu*[a] Jianzhuo Xin[a], Lei Wang[a], Jian-jun Song[a], Alex Y. S. Lee[b], and Paul Ho[a]

Received (in XXX, XXX) Xth XXXXXXXXX 20XX, Accepted Xth XXXXXXXXX 20XX

DOI: 10.1039/b000000x

We study the pyramid-like textured zinc oxide films from the low-temperature chemical bath deposition as a promising light trapping component in thin film silicon solar cells. It is found that the surface texture increases as the increase of film thickness, while the preferential orientation of crystal also changes gradually during the film growth. The textured zinc oxide film exhibits high transparency over 80% even for a relatively thick (e.g., 3.5 μm) film. Numerical modeling further indicates that the short circuit current of thin film microcrystalline silicon solar cell can be increased by 20% due to the light trapping effect arising from the textured zinc oxide film. Meantime, the sheet resistance of the as-grown textured zinc oxide film can be reduced drastically by hydrogen plasma treatment.

Introduction

It is well studied that light trapping is vital for efficient light harvesting in thin film solar cells.[1-5] The typical strategy for light trapping is to enhance light scattering and thus the effective optical path length in thin film solar cells. A variety of structures including pyramidal textured surface and nanowire arrays,[6-8] have been successfully fabricated for light trapping in photovoltaic devices. As for the thin film silicon solar cells, the transparent conductive oxide (TCO) with random pyramidal surface texture is usually employed for light trapping which is of paramount importance for the weakly absorbed light (800 nm to 1100 nm).[9-10] In comparison to other TCO, such as indium tin oxide (ITO) or fluorine doped tin oxide (FTO), zinc oxide (ZnO) is more preferable for production due to its abundance in the earth's crust and its lower cost. Moreover, ZnO exhibits higher hydrogen plasma resistance, which is essential for growth of silicon thin film using plasma enhanced chemical vapor deposition (PECVD).[11] Nowadays, industrial scale of high quality ZnO films can be obtained by using magnetron-sputtering or CVD methods,[9-13] although instrumental complexity requires high investment costs. In addition, some vacuum methods (e.g., magnetron-sputtering) would yield relatively flat ZnO film which needs further surface-texturing process (e.g., chemical wet-etching) to improve the light scattering capability.[12] Craters are usually formed by wet-etching sputtered aluminum doped ZnO (AZO) film, with predominantly small-angle scattering properties, which is less attractive for light trapping when compared with the Lambertian (cosine)-like angular resolved scattering from the pyramidal texture.[13-14] To this end, low cost non-vacuum approaches for fabrication of pyramid-like ZnO film with strong light scattering capability are of great interest for light trapping in thin film silicon solar cells.

In this work, we demonstrate a low-temperature solution method for the growth of pyramid-like ZnO film with strong light scattering capability to enhance the light absorption in thin film silicon solar cells. Similar with that obtained from the low-pressure CVD (LPCVD),[9] the feature size of pyramid and the scattering ability of ZnO film can be tuned by varying the thickness of ZnO film. To the best of our knowledge, no solution based pyramid-like ZnO film with relatively large surface texture has been reported before. Simulation results further indicate that the as-grown pyramid-like ZnO film substantially improves the quantum efficiency of microcrystalline thin film silicon solar cells at longer wavelength.

Experimental section

The pyramid-like ZnO film was prepared from the chemical bath deposition (CBD) on the glass substrates. Before the CBD process, a thin ZnO seed layer (~ 60 nm) was deposited on the glass by a sol-gel method.[15] The textured film deposition was carried out by immersing the seeded substrate in a solution of zinc acetate dehydrate and methenamine in a mixture of water and ethanol.[16] For a single step of growth, the solution was placed in a glass bottle which was kept in an oven at 80 ^{o}C for 4 hours. In order to increase the texture of the pyramid-like ZnO film and thus its light scattering capability, the same process was repeated one to four times. Due to large resistivity of intrinsic ZnO, a thin layer of highly transparent conductive film was deposited on top of the as-grown textured ZnO film to improve the electrical conductivity of the photovoltaic devices. As an example, a layer of 250 nm-thick AZO film was deposited on the thick pyramid-like ZnO (4x depositions) by rf-magnetron sputtering from ceramic target (2wt% Al_2O_3) at a pressure of 0.36 Pa and a substrtae temperature of 180 ^{o}C. The resistivity of the sputtered AZO film is around 5×10^{-4} Ω·cm which is comparable to the reported values of typical AZO film.[13] X-ray diffraction (XRD)

RSC Advances Accepted Manuscript

spectra of ZnO films were recorded with a Philiip X'pert instrument. The surface morphology and the cross-section of the textured ZnO films were chracterized using a Philips XL30 FEG scanning electron microscope (SEM). Ultraviolet-visible spectroscopy (UV-Vis) spectra were obtained at room temperature with an UV/vis spectrometer (Lambda 750) equipped with an integrating sphere. Finally, the effect of hydrogen plasma (120 mTorr, 300 W, 20 minutes) treatment was also studied as an alternative method to increase the conductivity of the as-grown textured ZnO film.

Results and discussion

The surface morphology of pyramid-like ZnO film with and without sputtered AZO was characterized by using SEM. As illustrated in Fig. 1(a), the feature size of pyramid (without sputtered AZO) from 4x deposition is larger than that of from 1x deposition (inset of Fig. 1(a)). The as-grown pyramid-like textured ZnO film via *n*x growth will be denoted as TZ-*n* (*n*=1~4) in the following context. Similar with that obtained from the LPCVD,[9] it is the pyramidal structure that gives to these ZnO films an surface texture, which would efficiently scatter the light. As shown in Fig. 1 (a), the basis size of the emerging pyramids for TZ-1 and TZ-4 are roughly 150 nm and 500 nm, respectively. The SEM surface morphology of TZ-4 with sputtered 250 nm-thick AZO film (AZO@TZ-4) and its corresponding cross-section are presented in Fig. 1(b) and its inset, respectively. The as-grown textured ZnO film has large crystal grains in its bulk without noticeable voids observed, indicating that light scattering would mainly occur at its textured surface. The thicknesses of TZ-1 and TZ-4 are around 0.5 μm and 3.5 μm, respectively, and the feature size of pyramid increases as the increase of film thickness. It is worth noting that the growth rate of film exhibits some variation in the deposition process, e.g., the thickness of TZ-1 and TZ-2 is around 0.5 μm and 1.5μm, respectively. Such variation is mainly due to the different substrate condition, i.e., the substrate with only the sol-gel based ZnO seeding layer differs significantly in growth rate with that after one step or two steps of textured ZnO growth. As will be discussed later, the growth rate is also related with the crystal orientations. The 250 nm-thick AZO film is almost conformal deposited on top of TZ-4, with certain nanoscale-texturing formed. Such nanoscale-texturing might cause antireflection and light scattering for light with shorter wavelength.[17]

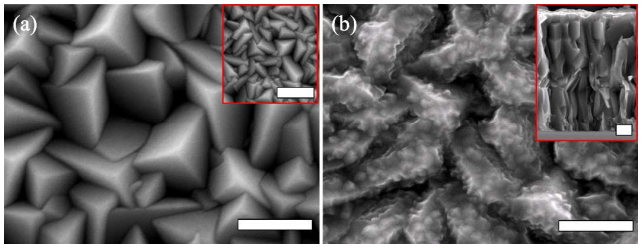

Fig. 1 (a) SEM surface morphology of TZ-4, with morphology of TZ-1 in the inset; (b) SEM surface morphology of AZO@TZ-4, with inset of its cross-section view. All scale bars in the figure 1 are 500 nm.

Besides the morphology variation, the crystal orientation of the as-grown textured ZnO film may also change significantly. The corresponding XRD spectra of the ZnO seed as well as the as-grown textured ZnO films are presented in Fig. 2. As illustrated, the diffraction peak of ZnO seed is extremely weak and thus diffraction signal mainly stems from the as-grown textured ZnO film. The diffraction peaks of as-grown textured ZnO film can be indexed to the hexagonal wurtzite structures (JCPDS card No. 79-2205). As for the TZ-1, it is preferentially oriented along the direction perpendicular to the (101) crystallographic plane. Surprisingly, as increase of the film thickness, the preferential orientation (the strongest diffraction peak) of the crystallite switches from (101) to (112), as depicted in Fig. 2. The crystal growth on the ZnO surfaces and hence the final shapes of the crystals are believed to be related with the solvent-solute interactions along different orientations of a crystal.[18-19] Since the surface atomic arrangement and thus the surface affinity for the solvent to each orientation is different, the growth rate on different crystal facet can be quite different. The evolution of orientation from (101) to (112) implies that crystal facet of (112) presents better surface affinity for the given solution than that of (101). While the preferential crystal orientation of (101) in TZ-1 is most likely due to the preferential crystal orientation of (101) in the seed layer as depicted in Fig. 2. As thickness increase, this original preferential orientation gradually disappears. Based on the (101) diffraction peak, the crystal size calculated from the Sherrer's equation yields a value of around 31 nm for these as-grown textured ZnO films, which is much smaller than the corresponding feature size of the pyramids. This discrepancy can be explained by the fact that the smallest crystals (including those in the seed-layer) at the bottom of the ZnO film are responsible for the observed broadening of the XRD peak, while crystals with large size have negligible contribution to the peak broadening.

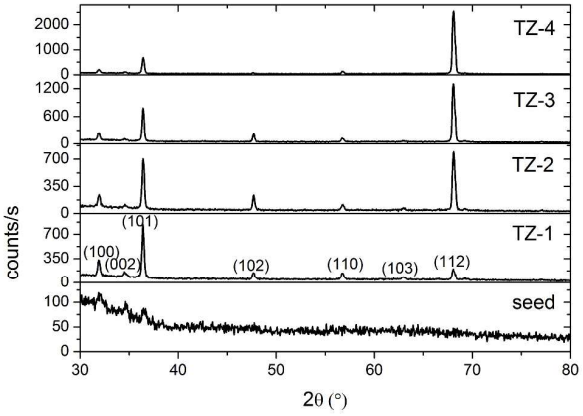

Fig.2 XRD spectra of as-grown textured TZ-n (n=1~4).

The transmission spectra of the textured ZnO films were obtained by using UV-Vis spectrometer equipped with an integrating sphere. As depicted in Fig. 3(a), the total transmission of TZ-1 and TZ-4 are around 85% and 80% in the spectral range from 500 to 1200 nm, respectively. Unlike the reduced transmission (~70% at 1100 nm) observed for the doped ZnO films,[20] the as-grown textured ZnO films exhibit high transparency even at longer wavelength, implying its low carrier concentration. The sputtered 250 nm-thick AZO on glass shows comparable transmission with that of TZ-1, while the transmission of AZO@TZ-4 is close to

RSC Advances Accepted Manuscript

This journal is © The Royal Society of Chemistry [year]

that of TZ-4. Fig. 3(b) illustrates the corresponding transmission haze as a function of wavelength defined as the ratio of diffuse transmission over the total transmission. As expected, the light scattering capability of the sputtered AZO film on glass is rather weak, with negligible transmission haze in the whole spectral range. As for the textured ZnO films, the light scattering capability significantly increases with thickness (or surface texture), as illustrated by the increase of corresponding transmission haze represented in Fig. 3(b). It's worth noting that the haze ratio of the as-grown textured ZnO film can be comparable to that of ZnO from LPCVD.[9] In addition, the transmission haze of AZO@TZ-4 is comparable with that of TZ-4, indicating that the as-grown ZnO textured film with sputtered AZO can be used as transparent electrode with strong light scattering capability. By using four-point probe measurement, it is found that the sheet resistance of sputtered AZO film on top of textured ZnO film is almost the same with that of sputtered AZO film on bare glass. It means that low sheet resistance (e.g., 10 Ω/sq) could be achieved for a relatively thick (e.g., 500 nm) AZO film sputtered on the as-grown textured ZnO film.

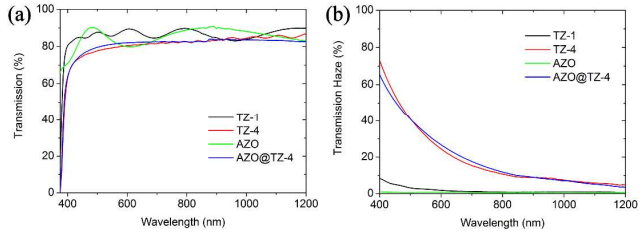

Fig. 3 Transmission spectra (a) and transmission haze (b) for TZ-1, TZ-4, AZO and AZO@TZ-4 (color online).

In order to study the effect of light trapping induced by the as-grown textured ZnO film on the optical performance of photovoltaic devices, we take AZO@TZ-4 as the front electrode in the thin film microcrystalline silicon (μcSi) solar cells as an example by means of ASA simulation.[21-23] The modeling parameters are mainly adapted from work by Ding *et al*.[23] Based on the scalar scattering theory,[22,24] light scattering at the rough interface of AZO@TZ-4/air or AZO@TZ-4/p-μcSi was described by using the atomic force microscopy image (not shown) of the AZO@TZ-4 as input in the ASA program. Fig. 4 (a) gives the refractive index (n) and the extinction coefficient (k) for the AZO film and TZ-4, respectively. For a better fitting of the total transmission spectra, the k value of both AZO film and TZ-4 was slightly modified based on the values in Ref. 23. As can be seen

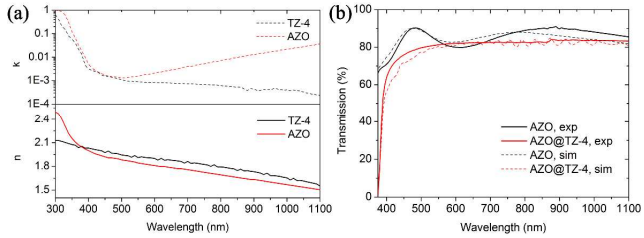

Fig. 4 (a) Refractive index of TZ-4 and AZO used in ASA simulation; (b) the measured and simulated transmission spectra of AZO and AZO@TZ-4 for comparison (color online).

in Fig. 4(b), the transmission spectra of 250 nm-thick AZO film and AZO@TZ-4 were more or less fitted. As for the 250 nm-thick AZO film deposited on the glass, we neglect the light scattering at the AZO/air interface due to its smooth nature which is evidenced from its transmission haze. In the simulation of thin film silicon solar cell, the following structure was used: glass (4 mm)/AZO (250 nm) or AZO (250 nm)@TZ-4(3.5 μm)/p-μcSi (20 nm)/i-μcSi (1200 nm)/n-μcSi (20 nm)/GZO (75 nm)/Ag (200 nm). In following context, the device with AZO and the device with AZO@TZ-4 as the front electrode will be denoted as D_AZO and D_AZO@TZ-4, respectively. Figures 5 (a) and 5 (b) show the absorption in each layer for D_AZO and D_AZO@TZ-4, respectively. As illustrated, the parasitic absorption in D_AZO@TZ-4 is larger than that in D_AZO for spectral range from 300 nm to 450 nm, as a result of the introduction of TZ-4. The distinct interference pattern presented in Fig. 5 (a) arises from the coherent nature of specular light in the device (D_AZO) with flat interfaces, while it was alleviated remarkably for D_AZO@TZ-4 due to the strong light scattering at the rough interface, as shown in Fig. 5(b). The corresponding simulated external quantum efficiency (EQE) of device is depicted in Fig. 5(c). The effect of sheet resistance of front electrode on the efficiency of current collection was not taken into account, since this simulation mainly focuses on the optical performance. Light absorbed in the layer of i-μcSi contributes to the major part of photocurrent in the devices, while the absorption in the doped silicon layers produces negligible photocurrent. Similar to the optical absorption in the layer of i-μcSi, the average EQE of textured device is larger than that of flat device in spectral range from 650 nm to 1100 nm (see Fig. 5 (c)), although it is relative lower at short wavelength from 350 nm to 450 nm due to the aforementioned enhanced parasitic absorption from the TZ-4. As a result, the short circuit current density (J_{SC}) estimated from the

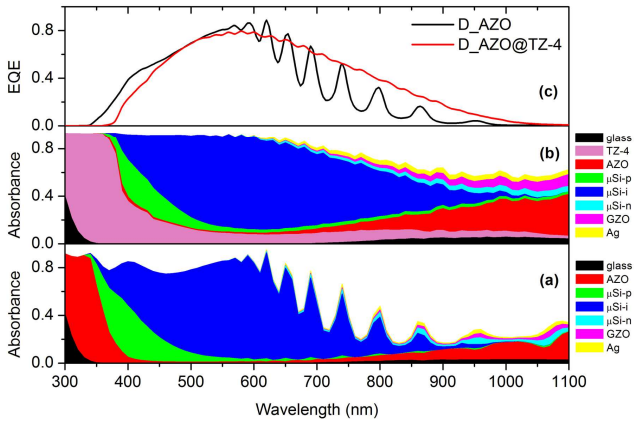

Fig. 5 (a) simulated layer-absorption in D_AZO; (b) simulated layer-absorption in D_AZO@TZ-4; and (c) simulated external quantum efficiency of D_AZO and D_AZO@TZ-4 (color online). The thickness of i-μcSi is 1200 nm.

corresponding EQE is 18.6 mA/cm^2 and 15.5 mA/cm^2 for D_AZO@TZ-4 and D_AZO, respectively (corresponding to 20% enhancement). In order to verify the effect of enhanced light scattering on different thickness of light absorption layer, we also changed the thickness of i-μcSi layer from 800 nm to 1600 nm in

RSC Advances Accepted Manuscript

ASA simulation. The improvement in J_{SC} is 23% and 17% for i-μcSi with thickness of 800 nm and 1600 nm, respectively. This implies that the as-grown textured ZnO film can significantly improve the photocurrent of thin film silicon solar cells due to its strong light trapping effect. The simulated *J-V* characteristics of devices with different thickness of i-μcSi are summarized in Table 1.

Table 1. The simulated *J-V* characteristics of devices with different thickness of i-μcSi and two TCO configurations, with J_{SC} short circuit current density, V_{OC} the open circuit voltage, *FF* the fill factor, *PCE* the power conversion efficiency.

$t_{i\text{-}\mu cSi}$(nm)	TCO	J_{sc} (mA/cm^2)	V_{OC} (V)	*FF* (%)	*PCE* (%)
800	AZO	13.9	0.54	76.4	5.73
	AZO@TZ-4	17.2	0.55	75.2	7.08
1200	AZO	15.5	0.53	72.3	5.91
	AZO@TZ-4	18.6	0.53	71.0	7.07
1600	AZO	16.7	0.52	69.7	6.05
	AZO@TZ-4	19.5	0.53	68.9	7.06

As for the front electrode, low sheet resistance (< 15 Ω/sq) is critical in practical photovoltaic devices. Besides the aforementioned sputtered AZO coating, simple treatments, such as UV-light or hydrogen plasma,[25-26] can also be employed to reduce the sheet resistance of as-grown textured ZnO films, which would be a more cost-effective way to fabricate highly transparent conductive ZnO films when combined with the low-temperature solution growth approach. In our initial experiment, hydrogen plasma was used to treat one of the as-grown samples (TZ-2), which results in a substantial decrease of sheet resistance from an initial value of 2.37×10^8 Ω/sq to 170 Ω/sq. By fine turning the treatment process, lower sheet resistance could be achieved. Both the increased concentration of oxygen vacancies and the reduced density of electron traps at the grain boundaries might be responsible for the improvement of conductivity.[27] Furthermore, the hydrogen plasma treatment used in this work has negligible influence on the optical absorbance of the textured ZnO films in the region of interest (300 nm to 1100 nm), which is consistence with the results obtained in the work of Ding *et al*.[27] Besides the texturing of the front TCO, the as-grown textured ZnO films presented in this work may also be used in texturing of back-TCO of thin film silicon solar cells.[28-29] Moreover, the low-temperature solution growth of textured ZnO films is compatible for deposition of thin film silicon solar cells on flexible plastic substrates such as polyethylene-terephtalate (PET) or polyethylene-naphtalate (PEN), making it attractive for other potential light trapping applications.

Conclusions

We demonstrated the solution growth of textured ZnO films with pyramidal surface morphology, which have tunable light scattering capability and can be used in thin film silicon solar cells for efficient light trapping. The surface texture of the as-grown ZnO films increases with the increase of their thickness, and the preferential crystal orientation of textured ZnO film also gradually changes from (101) to (112). By means of ASA simulation, strong light trapping effect from the textured ZnO film was further verified in thin film microcrystalline silicon solar cells, with an increase of short circuit current density of more than 20%. Furthermore, the conductivity of the as-grown textured ZnO film could be significantly increased by simple hydrogen plasma post-treatment. Such solution based ZnO film with strong light scattering capability has great potential in the development of thin film solar cells.

ACKNOWLEDGMENT

This work was supported by Innovation Technology Commission of Hong Kong (ITP/044/12NI).

Notes and references

[a] *Nano and Advanced Materials Institute Limited, The Hong Kong University of Science and Technology, Hong Kong SAR, P.R.China*
E-mail: liuchaoping7281@hotmail.com
[b] *DuPont Apollo Limited, Hong Kong SAR, P. R. China.*

1 B. Janthong, Y. Moriya, A. Hongsingthong, P. Sichanugrist, and M. Konagai, *Solar Energy Materials and Solar Cells*, 2013, **119**, 209-213.
2 J. Escarré, K Söderström, M. Despeisse, S. Nicolay, C. Battaglia, G. Bugnon, L. Ding, F. Meillaud, F. J. Haug, and C. Ballif, *Solar Energy Materials and Solar Cells*, 2012, **98**, 185-190.
3 M. Vanecek, O. Babchenko, A. Purkrt, J. Holovsky, N. Neykova, A. Poruba, Z. Remes, J. Meier, and U. Kroll, *Appl. Phys. Lett.*, 2011, **98**, 163503.
4 C. P. Liu, Z. H. Chen, H. E. Wang, S. K. Jha, W. J. Zhang, I. Bello, and J. A. Zapien, *Appl. Phys. Lett.*, 2012, **100**, 243102.
5 S. W. Baek, J.Noh, C. H. Lee, B. S. Kim, M. K. Seo, and J. Y. Lee, *Scientific Reports*, 2013, **3**, 1726.
6 P. Cambell, and M. A. Green, *J. Appl. Phys.*, 1987, **62**, 243-249.
7 R. Rothemund, T. Umundum, G. Meinhardt, K. Hingerl, T. Fromherz, and W. Jantsch *Prog. Photovolt: Res. Appl.*, 2013, **21**, 747-753.
8 E. C. Garnett, M. L. Brongersma, Y. Cui, and M. D. McGehee, *Annu.Rev. Mater. Res.*, 2011, **41**, 269-295.
9 S. Faÿ, L. Feitknecht, R. Schlüchter, U. Kroll, E. V. Sauvain, and A. Shah, *Solar Energy Materials and Solar Cells*, 2006, **90**, 2960-2967.
10 S. Hänni, G. Bugnon, G. Parascandolo, M. Boccard, J. Escarré, M. Despeisse, F. Meillaud, and C. Ballif, *Prog. Photovolt: Res. Appl.*, 2013, **21**, 821-826.
11 T. Ikeda, K. Sato, Y. Hayashi, Y. Wakayama, K. Adachi, and H. Nishimura, *Solar Energy Materials and Solar Cells*, 1994, **34**, 379-384.
12 J. Müller, B. Rech, J. Springer, and M. Vanecek, *Solar Energy*, 2004, **77**, 917-930.
13 M. Berginski, J. Hüpkes, W. Reetz, B. Rech, M. Wuttig, *Thin Solid Films*, 2008, **516**, 5836-5841.
14 H. Schade, P. Lechner, R. Geyer, H. Stiebig, B. Rech, and O. Kluth, *Conference Record of the 31th IEEE*, 2005, 1436-1439.
15 C. P. Liu, H. E. Wang, T. W. Ng, Z. H. Chen, W. F. Zhang, C. Yan, Y. B. Tang, I. Bello, L. Martinu, W. J. Zhang, and S. K. Jha, *Phys. Status Solidi B*, 2012, **249**, 627-633.
16 M. Wang, E. J. Kim, E. W. Shin, J. S. Chung, S. H. Hahn, and C. Park, *J. Phys. Chem. C*, 2008, **112**, 1920-1924.
17 M. Beccard, P. Cuony, C. Battaglia, S. Hänni, S. Nicolay, L. Ding, M. Benkhaira, G. Bugnon, A. Billet, M. Charrière, K. Söderström, J. Escarrè, F. S. Meillaud, M. Despeisse, and C. Ballif, *IEEE Journal of Photovoltaics*, 2012, **2**, 83-87.
18 S. Baruah, and J. Dutta, *Sci.Technol. Adv. Mater.*, 2009, **10**, 013001.
19 G. Liu, J. C. Yu, G. Q. Lu, and H. M. Cheng, *Chem. Commun.*, 2011, **47**, 6763-6783.
20 K. L. Chopra, S. Major, D. K. Pandya, *Thin Solid Films*, 1983, **102**, 1-46.

RSC Advances Accepted Manuscript

This journal is © The Royal Society of Chemistry [year]

21 B. E. Pieters, J. Krč, M. Zeman, Advanced numerical simulation tool for solar cells-ASA5, in: *Proceedings of the 4th WCPEC*, 7-12 May, Waikoloa, Hawaii, 2006, pp. 1513-1516.

22 M. Zeman, O. Isabella, S. Solntsev, K. Jäger, *Solar Energy Materials and Solar Cells*, 2013, **119**, 94-111.

23 K. Ding, T. Kirchartz, B. E. Pieters, C. Ulbrich, A. M. Ermes, S. Schicho, A. Lambertz, R. Carius, and U. Rau, *Solar Energy Materials and Solar Cells*, 2011, **95**, 3318-3327.

24 M. Born, E. Wolf, Principles of Optics, 7th edition, Cambridge University Press, ISBN 978-0-5216-4222-4, 1999.

25 A. Yamada, W. W. Wenas, M. Yoshino, M. Konagai, and K. Takahashi, *Jpn. J. Appl. Phys.*, 1991, **30**, L1152-L1154.

26 H. Hagendorfer, K. Lienau, S. Nishiwaki, C. M. Fella, L. Kranz, A. R. Uhl, D. Jaeger, L. Luo, C. Gretener, S. Buecheler, Y. E. Romanyuk, and A. N. Tiwari, *Adv. Mater.*, 2014, **26**, 632-636.

27 L. Ding, S. Nicolay, J. Steinhauser, U. Kroll, and C. Ballif, *Adv. Funct. Mater.*, 2013, **23**, 5177-5182.

28 T. Söderstöm, F. J. Haug, X. Niquille, and C. Ballif, Prog. *Photovolt: Res. Appl.*, 2009, **17**, 165-176.

29 C. Hsu, C. Battaglia, C. Pahud, Z. Ruan, F. J. Haug, S. Fan, C. Ballif, and Y. Cui, *Adv. Energy Mater.*, 2012, **2**, 628-633.

RSC Advances Accepted Manuscript